

# All-Organic Discotic Radical with a Spin-Carrying Rigid-Core Showing Intracolumnar Interactions and Multifunctional Properties\*\*

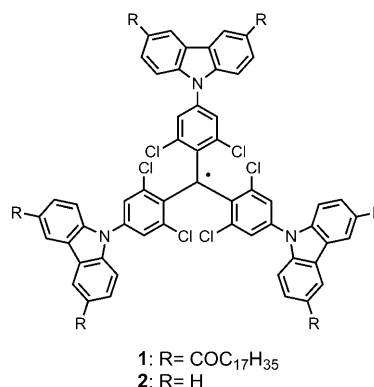
Sonia Castellanos, Francisco López-Calahorra, Enric Brillas, Luis Juliá,\* and Dolores Velasco\*

The ability of liquid crystals (LCs) to rearrange and thus modify their physical properties as a response to an external stimulus, such as light incidence, temperature changes, or the application of an electrical or magnetic field, is a useful feature for technological applications. Discotics are especially interesting from the point of view of the development of semiconductor devices because of their ability to form one-dimensional superstructures that allow free electric charges to migrate. This feature has been recognized as an attractive property for the construction of light-emitting diodes, photovoltaic cells, and field-effect transistors.<sup>[1]</sup> In particular, carbazole derivatives play an important role as organic materials for electronic applications.<sup>[2]</sup> However, not many carbazole-containing discotic LCs have been reported to date.<sup>[1a,3,4]</sup>

The development of spin systems with LC properties is particularly interesting in the field of magnetism because of the possibility of altering the magnetic properties through the phase transition, or the modulation of the magnetic response by external fields.<sup>[5–23]</sup> Some calamitic all-organic radical LCs containing 2,2,6,6-tetramethylpiperidine-*N*-oxide and 2,2,5,5-tetramethyl-1-pyrrolidine-*N*-oxide as spin sources,<sup>[10–13,21,22]</sup> which can be ordered into a variety of LC nematic or layered phases, can be found in the literature. However, there is only one example of a disk-like all-organic radical that has the spin-supporting unit introduced into the disk-like triphenylene core as a lateral chain-bonded moiety.<sup>[23]</sup>

With this in mind, we have developed a new discotic all-organic LC with a radical rigid core based on the tris[4-(*N*-

carbazolyl)-2,6-dichlorophenyl]methyl aromatic system.<sup>[24]</sup> Free radicals of the tris(2,4,6-trichlorophenyl)methyl (TTM) series are very persistent species both in the solid state and in solution owing to the presence of the very bulky polychlorophenyl substituents around the trivalent carbon atom.<sup>[25]</sup> In particular, radical adducts based on carbazoyl TTM radical exhibit electrochemical amphotericity and remarkable luminescent properties into the visible range of the electronic spectrum.<sup>[24,26,27]</sup> To the best of our knowledge, the radical adduct presented herein is the first disk-like LC with the magnetic spin source placed in the center of the rigid discotic core.



The novel radical adduct **1** was obtained by the direct Friedel–Crafts acylation of tris[4-(*N*-carbazolyl)-2,6-dichlorophenyl]methyl radical **2** (see the Supporting Information). The presence of the long acyl chains in the carbazole moiety provides the new radical with the typical features of a disk-like mesogen. Radical **1** does not crystallize, and exhibits different columnar phases that were studied by optical, calorimetric, and diffractometric methods.

In the differential scanning calorimetry (DSC) curve, a peak at 351 K is observed during cooling from the isotropic state to lower temperatures (Figure 1). This peak corresponds to the formation of an ordered hexagonal columnar (Col<sub>ho</sub>) mesophase, as shown by X-ray diffraction (XRD) analysis at 333 K (Supporting Information, Figure S1).<sup>[28]</sup> A second peak covers a broad range of temperatures from 300 K to 274 K. No crystallization is associated to this peak, but rather a vitrification of a rectangular columnar mesophase. The new phase showed a lack of fluidness by polarized optical microscopy (POM), and gave rise to an X-ray diffractogram that is in accord with a two-dimensional lattice structure with a rectangular arrangement (Supporting Information, Figure S2). The symmetric profile of the DSC analyses of **1**

[\*] S. Castellanos, Dr. L. Juliá  
Departament de Química Biològica i Modelització Molecular  
Institut de Química Avançada de Catalunya (CSIC)  
Jordi Girona, 18-26, 08034 Barcelona (Spain)  
E-mail: ljbmo@cid.csic.es

Prof. F. López-Calahorra, Dr. D. Velasco  
Departament de química Orgànica, Institut de Nanociències i  
Nanotecnologia, Universitat de Barcelona  
Martí i Franquès 1-11, 08028 Barcelona (Spain)  
E-mail: dvelasco@ub.edu

Prof. E. Brillas  
Departament de Química Física, Universitat de Barcelona  
Martí i Franquès 1-11, 08028 Barcelona (Spain)

[\*\*] Financial support for this research was obtained from the Ministerio de Educación y Ciencia (Spain) through grant no. CTQ2006-15611-C02-02/BQU. S.C. is gratefully acknowledged to the Generalitat de Catalunya for a predoctoral grant. We also thank the EPR service of the Institut de Ciència de Materials de Barcelona (CSIC) for recording the EPR spectra.

Supporting information for this article is available on the WWW under <http://dx.doi.org/10.1002/anie.200902641>.

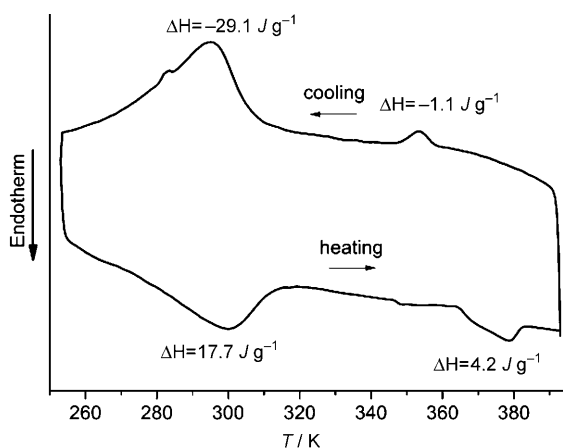


**Figure 1.** DSC curves of **1** (cooling and heating) from 253 K to 393 K, at a rate of 10 K min<sup>-1</sup>.

during the second heating process indicates the enantiotropic character of the mesophase. Table 1 summarizes the indexing of the diffractogram corresponding to both columnar mesophases.

**Table 1:** Indexation of XRD profiles at given temperatures of the found phases.<sup>[a]</sup>

T [K]	Phase	d [Å]	Miller indices (hkl)	Lattice parameters [Å]
253	Col <sub>r</sub>	40.2	200	a = 80.4
		34.6	110	b = 38.3
		20.1	400	
		4.3		
333	Col <sub>ho</sub>	43.1	100	a = 49.8
		25.6	110	c = 3.5
		21.5	200	
		14.4	300	
		8.5	500	
		7.2	600	
		6.1	700	
		4.5		
		3.5	001	

[a] Col<sub>r</sub> = glassy rectangular columnar; Col<sub>ho</sub> = ordered hexagonal columnar mesophase.

Homeotropic alignment during the cooling from the isotropic state of radical adduct **1** was observed by using POM<sup>[29]</sup> at 333 K (Supporting Information, Figure S3). The sample was uniformly black when polarizers were crossed, and birefringence could only be observed when pressure was applied to the sample. Though the transition between Col<sub>r</sub> and Col<sub>ho</sub> was detected by DSC analyses, no changes in the texture associated to the phase transition were recorded by POM during the cooling or the heating processes.

Given the homeotropic alignment of the columnar hexagonal phase and its intracolumnar core–core interactions, the magnetic intermolecular interactions in the mesophase were investigated. The magnetic susceptibility of radical adduct **1** was measured on a SQUID MPMS-XL Quantum Design (5 T) over the temperature range 2–400 K (Figure 2).

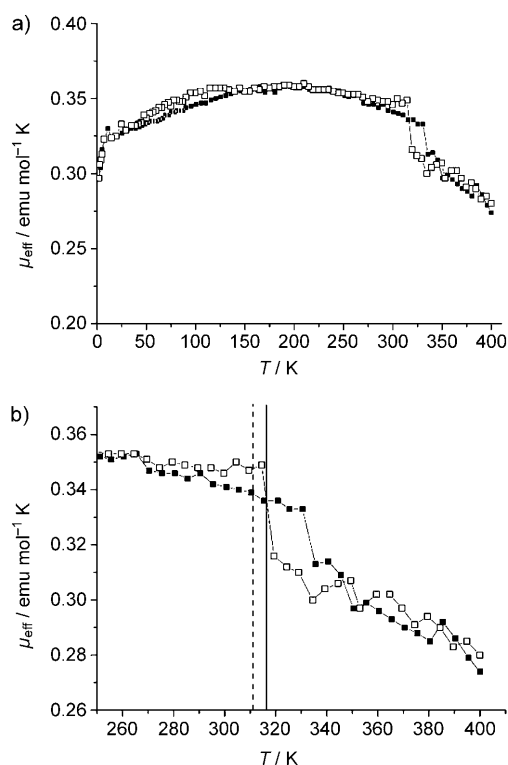


**Figure 2.** Temperature dependence of the effective magnetic moment ( $\mu_{\text{eff}}$ ) of radical **1** during the cooling ( $\square$ ) and the second heating process ( $\blacksquare$ ) at a rate of 10 K min<sup>-1</sup>. a) Dependence between 2 and 400 K at a field of 5 T; b) a detailed plot of the function between 250 and 400 K. The dashed line indicates the temperature at which the Col<sub>ho</sub> phase disappears during the cooling process; the continuous line indicates the temperature at which Col<sub>ho</sub> phase is completely formed during the heating process according to DSC analyses.

Radical **1** shows an increase in  $\mu_{\text{eff}}$  from 0.32 to 0.35 at 313 K during cooling from the isotropic liquid state, which is in agreement with the beginning of the exothermic peak in the DSC analysis (ca. 310 K), and thus coinciding with the transition to the rectangular glassy state from the Col<sub>ho</sub> phase. The new value  $\mu_{\text{eff}} \approx 0.35$  corresponds to the value of a monoradical ( $S = 1/2$ ;  $\mu_{\text{eff}} = 0.37$ ), and suggests that the core–core interaction deduced from the diffraction peak at 3.5 Å found in this phase has an antiferromagnetic character. Values of  $\mu_{\text{eff}}$  remain constant during the glassy rectangular phase until it decreases drastically from  $T \approx 20$  owing to strong antiferromagnetic interactions. A reversibility of the magnetic interactions is observed during the second heating from 2 K. A drop in the  $\mu_{\text{eff}}$  values from 0.35 to 0.31 at approximately 330 K, where the transition from the glassy Col<sub>r</sub> phase to the Col<sub>ho</sub> mesophase is fully completed, indicates the reappearance of the intermolecular antiferromagnetic interactions between neighboring molecules in the columnar packing. This reversible magnetic behavior is also seen in the identical values of the Curie constant  $C$  and the Weiss temperature  $\theta$  obtained in the heating and the cooling processes (Table 2).

To confirm that the changes of the magnetic intermolecular interaction could be assigned unequivocally to the core–core interaction in the ordered Col<sub>ho</sub> phase, the Landé  $g$  value

**Table 2:** Magnetic susceptibility data of radical **1**.

Process	Magnetic interactions	C [emu mol <sup>-1</sup> K <sup>-1</sup> ] <sup>[a]</sup>	$\theta$ [K] <sup>[a]</sup>	Phase transition [K] <sup>[b]</sup>
cooling	antiferromagnetic	0.34	-0.30	Col <sub>r</sub> 265–308 Col <sub>ho</sub> 348–359 (I)
heating	antiferromagnetic	0.34	-0.30	Col <sub>r</sub> 299–316 Col <sub>ho</sub> 364–383 (I)

[a] Values obtained from the magnetic susceptibility curves registered over the 2–400 K range. [b] Transition temperatures determined by DSC analysis between the different found states: glassy rectangular state (Col<sub>r</sub>), ordered hexagonal columnar mesophase (Col<sub>ho</sub>), and isotropic state (I).

and the band intensity and linewidth values of the band in the electron paramagnetic resonance (EPR) spectrum of the radical **1** were registered as a function of the temperature. The spectra were recorded during the cooling process from the isotropic melted state (400 K) to the Col<sub>r</sub> mesophase (230 K) and during the second heating process going from the Col<sub>r</sub> to the Col<sub>ho</sub> mesophases (300 K) (Figure 3). The  $g$  value only showed a slight increase from 2.0026 to 2.0032 during the cooling process and then remained almost constant during the heating. As a general rule, polychlorotriphenylmethyl radicals have axial symmetry with anisotropic  $g$  values:  $g_{\perp} = 2.0019 \pm 0.0004$  and  $g_{\parallel} = 2.00046 \pm 0.0005$ . Considering that the  $g_{\parallel}$

component is set along the semi-occupied 2p orbital of the trivalent carbon, the small increase in  $g$  might be attributed to a slight major contribution of the  $g_{\parallel}$ . Therefore, once molecules form columns from the melted isotropic state, they do not experience changes in their orientation during the phase transitions and tend to align the 2p orbital closer to the direction of the magnetic field.

Whereas the intensity of the band in the EPR spectrum of **1** increased with decreasing temperature from 400 K to 220 K according to the Curie's law, the linewidth dropped in an almost linear rate in the range 400–340 K, corresponding to the isotropic state, owing to an increase of the spin-relaxation times with the decrease in temperature (Figure 3b). Below 340 K, the linewidth became constant, indicating a stabilization of the relaxation time that can be attributed to the formation of the columnar mesophase. In particular, molecules occupy positions in a columnar order, in which the intracolumnar core–core interaction and the spin-relaxation mechanisms remain unaltered within the temperature range in which this intracolumnar order is preserved. After the Col<sub>ho</sub>→Col<sub>r</sub> transition, however, linewidth values increased slightly in the temperature range in which magnetic susceptibility values indicate a monoradical behavior and thus the loss of intermolecular intracolumnar interactions. The intensity and linewidth values are reproduced during the second heating as a consequence of the enantiotropic character of the phases.

The presence of an unpaired electron in the core of the molecule is not only interesting because of the magnetic properties its paramagnetic character can provide. The electronic properties can derive from the existence of the semi-occupied molecular orbital (SOMO) that contains this single electron, which according to the EPR studies is mainly located on the trivalent carbon (see the Supporting Information for analyses of Figure S4) and theoretical calculations.<sup>[26]</sup> Therefore, electrochemical and photoluminescence properties of the new radical adduct **1** were studied by cyclic voltammetry and absorption and emission UV/Vis spectra, respectively.

The cyclic voltammogram (CV) of **1** in CH<sub>2</sub>Cl<sub>2</sub> (10<sup>-3</sup> M) displayed two quasi-reversible redox pairs (see the Supporting Information, Figure S5 and S6); one corresponding to its reduction ( $\mathbf{1} \rightleftharpoons \mathbf{1}^{-\bullet}$ ),  $E^{\circ}(\mathbf{A}^{\bullet}/\mathbf{A}^{-}) = -0.39$  V versus the saturated calomel electrode (SCE), and the other one to its oxidation ( $\mathbf{1}^{\bullet} \rightleftharpoons \mathbf{1}^{+}$ ),  $E^{\circ}(\mathbf{A}^{+}/\mathbf{A}^{\bullet}) = 1.12$  V vs. SCE. The electron affinity (EA = 4.3 eV) and ionization potential values (IP = 5.7 eV) of the radical were estimated on the basis of the reference energy level of ferrocene (4.8 eV below the vacuum level)<sup>[30]</sup> according to the formula  $\text{IP}/\text{AE} = 4.8 + E^{\text{onset}} - E^{\circ}(\text{Fc}/\text{Fc}^{+})$  eV, where  $E^{\text{onset}}$  are the onset potentials for oxidation (1.04 V) and reduction (-0.30 V) of radical **1** versus SCE, respectively, and where  $E^{\circ}(\text{Fc}/\text{Fc}^{+}) = 0.16$  V is the redox potential for the oxidation of ferrocene versus SCE.

The UV/Vis absorption spectrum of radical adduct **1** in CHCl<sub>3</sub> solution (10<sup>-4</sup> M) showed a wide light-absorption range from the UV to the red region of the visible spectrum. Four main bands were observed (Supporting Information, Figure S7).<sup>[31]</sup> The shoulder at 550 nm, which is partly masked by a weak charge-transfer band from the carbazole to the

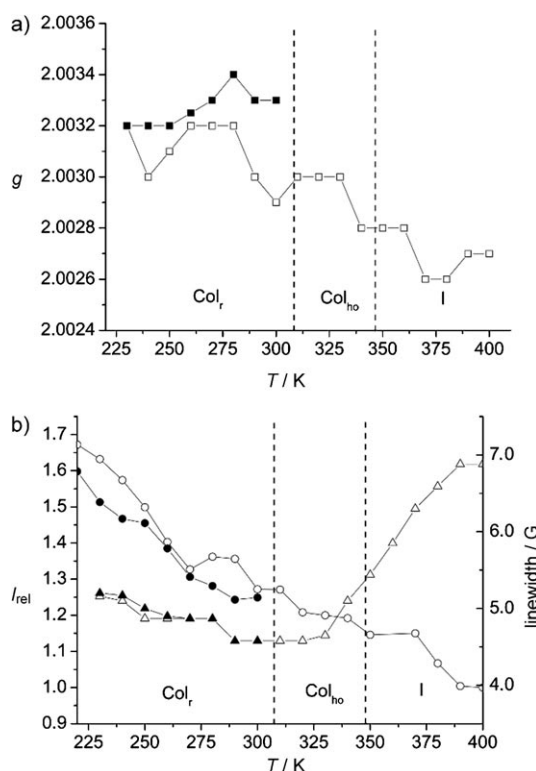


**Figure 3.** a) Variation of  $g$  (■,□) and b) the band intensity (●,○) and the band linewidth values (▲,△) in the EPR spectra of radical **1** during the cooling process from the isotropic melted state (open symbols) and the second heating process (filled). Dashed lines delineate the Col<sub>ho</sub> phase temperature ranges determined by DSC analysis during the cooling process.

trivalent carbon at 593 nm, is assigned to the SOMO  $\rightarrow$  LUMO ( $n \rightarrow \pi^*$ ) transition, and thus  $E_{\text{gap}}$  is estimated to be 2.2 eV. Cyclohexane and chloroform solutions of radical **1** showed intense bands in the visible region of the emission spectra in both solvents, with maxima at 631 nm in cyclohexane and at 642 nm in chloroform, and quantum efficiencies of  $\theta = 0.34$  and  $\theta = 0.31$ , respectively (Supporting Information, Figure S7).

In summary, the first paramagnetic all-organic disk-like liquid crystal has been synthesized that localizes the unpaired electron in the center of the aromatic core. This compound has two enantiotropic columnar phases: a glassy rectangular columnar phase at low temperatures and an ordered hexagonal columnar mesophase above room temperature. Core–core interactions and their derived magnetic interactions during the Col<sub>ho</sub> mesophase have been detected by several techniques. This new radical adduct has advantageous electrochemical and photoluminescence characteristics for its application in electronic devices, such as absorption in the visible spectrum, emission in the red region of the visible spectrum, and ambipolar redox properties owing to the existence of the SOMO in which the single electron mainly resides.

Received: May 18, 2009  
Published online: July 23, 2009

**Keywords:** electrochemistry · EPR spectroscopy · fluorescence · liquid crystals · magnetic properties

- [1] a) M. J. Sienkowska, H. Monobe, P. Kaszynski, Y. Shimizu, *J. Mater. Chem.* **2007**, *17*, 1392–1398; b) S. Sergeyev, W. Pisulab, Y. H. Geerts, *Chem. Soc. Rev.* **2007**, *36*, 1902–1929; c) H. Iino, J.-I. Hanna, R. J. Bushby, B. Movaghar, B. J. Whitaker, *J. Appl. Phys.* **2006**, *100*, 043716; d) M. Kastler, F. Laquai, K. Mullen, G. Wegner, *Appl. Phys. Lett.* **2006**, *89*, 252103; e) C. Deibel, D. Janssen, P. Heremans, V. De Cupere, Y. Geerts, M. L. Benkheldir, G. J. Adriaenssens, *Org. Electron.* **2006**, *7*, 495–499; f) H. Iino, J.-I. Hanna, R. J. Bushby, B. Movaghar, B. J. Whitaker, M. J. Cook, *Appl. Phys. Lett.* **2005**, *87*, 132102; g) J. Piris, M. G. Debije, N. Stutzmann, A. M. van de Craats, M. D. Watson, K. Mullen, J. M. Warman, *Adv. Mater.* **2003**, *15*, 1736–1740; h) I. Seguy, P. Destruel, H. Bock, *Synth. Met.* **2000**, *111–112*, 15–18.
- [2] a) J. V. Grazulevicius, P. Stroehriegel, J. Pielichowski, K. Pielichowski, *Prog. Polym. Sci.* **2003**, *28*, 1297–1353; b) K. Parimal, K. R. Justin Thomas, T. L. Jiann, Y. T. Tao, C. H. Chien, *Adv. Funct. Mater.* **2003**, *13*, 445–452; c) B. Akira, O. Ken, K. Wolfgang, C. A. Rigoberto, *J. Phys. Chem. B* **2004**, *108*, 18949–18955; d) A. van Dijken, J. J. A. M. Bastiaansen, N. M. M. Kiggen, B. M. W. Langeveld, C. Rothe, A. Monkman, I. Bach, P. Stössel, K. Brunner, *J. Am. Chem. Soc.* **2004**, *126*, 7718–7727; e) J. F. Morin, N. Drolet, Y. Tao, M. Leclerc, *Chem. Mater.* **2004**, *16*, 4619–4626; f) K. R. Justin Thomas, M. Velusamy, J. T. Lin, Y. T. Tao, C. H. Chuen, *Adv. Funct. Mater.* **2004**, *14*, 387–392; g) K. Brunner, A. V. van Dijken, H. Börner, J. J. A. M. Bastiaansen, N. M. M. Kiggen, B. M. W. Langeveld, *J. Am. Chem. Soc.* **2004**, *126*, 6035–6042; h) M.-H. Tsai, Y.-H. Hong, C.-H. Chang, H.-C. Su, C.-C. Wu, A. Matoliukstyte, J. Simokaitiene, S. Grigalevicius, J. V. Grazulevicius, C.-P. Hsu, *Adv. Mater.* **2007**, *19*, 862–866.
- [3] M. Manickam, M. Belloni, S. Kumar, S. K. Varshney, D. S. Shankar Rao, P. R. Ashton, J. A. Preece, N. Spencer, *J. Mater. Chem.* **2001**, *11*, 2790–2800.
- [4] a) E. Perea, F. Lopez-Calahorra, D. Velasco, *Liq. Cryst.* **2002**, *29*, 421–428; b) E. Perea, F. López-Calahorra, D. Velasco, H. Finkelmann, *Mol. Cryst. Liq. Cryst.* **2001**, *365*, 695–702.
- [5] D. Sy, A. Sanson, M. Ptak, *Solid State Commun.* **1972**, *10*, 985–988.
- [6] R. Tamura, S. Susuki, N. Azuma, A. Matsumoto, F. Toda, Y. Ishii, *J. Org. Chem.* **1995**, *60*, 6820–6825.
- [7] D. Ionescu, G. R. Luckhurst, D. S. DeSilva, *Liq. Cryst.* **1997**, *23*, 833–843.
- [8] M. Mizumoto, H. Ikemoto, H. Akutsu, J. I. Yamada, S. Nakatsuji, *Mol. Cryst. Liq. Cryst.* **2001**, *363*, 149–156.
- [9] S. Nakatsuji, *Adv. Mater.* **2001**, *13*, 1719–1724.
- [10] M. Mazzoni, L. Franco, A. Ferrarini, C. Corvaja, G. Zordan, G. Scorrano, M. Maggini, *Liq. Cryst.* **2002**, *29*, 203–208.
- [11] S. Nakatsuji, M. Mizumoto, H. Ikemoto, H. Akutsu, J.-I. Yamada, *Eur. J. Org. Chem.* **2002**, *12*, 1912–1918.
- [12] S. Nakatsuji, H. Ikemoto, H. Akutsu, J. Yamada, A. Mori, *J. Org. Chem.* **2003**, *68*, 1708–1714.
- [13] N. Ikuma, R. Tamura, S. Shimono, N. Kawame, O. Tamada, N. Sakai, J. Yamauchi, Y. Yamamoto, *Angew. Chem.* **2004**, *116*, 3763–3768; *Angew. Chem. Int. Ed.* **2004**, *43*, 3677–3682.
- [14] N. Ikuma, R. Tamura, K. Masaki, Y. Uchida, S. Shimono, J. Yamauchi, Y. Aoki, H. Nohira, *Ferroelectrics* **2006**, *343*, 119–125.
- [15] Y. Noda, S. Shimono, M. Baba, J. Yamauchi, N. Ikuma, R. Tamura, *J. Phys. Chem. B* **2006**, *110*, 23683–23687.
- [16] M.-Y. Zheng, Z.-W. An, *Chin. J. Chem.* **2006**, *24*, 1754–1757.
- [17] M. J. Sienkowska, J. M. Farrar, P. Kaszynski, *Liq. Cryst.* **2007**, *34*, 19–24.
- [18] Y. Uchida, R. Tamura, N. Ikuma, S. Shimono, J. Yamauchi, Y. Aoki, H. Nohira, *Mol. Cryst. Liq. Cryst.* **2007**, *479*, 1251–1259.
- [19] J. Zienkiewicz, A. Fryszkowska, K. Zienkiewicz, F. Guo, P. Kaszynski, A. Januszko, D. Jones, *J. Org. Chem.* **2007**, *72*, 3510–3520.
- [20] Y. Noda, S. Shimono, M. Baba, J. Yamauchi, Y. Uchida, N. Ikuma, R. Tamura, *Appl. Magn. Reson.* **2008**, *33*, 251–267.
- [21] R. Tamura, Y. Uchida, N. Ikuma, *J. Mater. Chem.* **2008**, *18*, 2872–2876.
- [22] Y. Uchida, N. Ikuma, R. Tamura, S. Shimono, Y. Noda, J. Yamauchi, Y. Aoki, H. Nohira, *J. Mater. Chem.* **2008**, *18*, 2950–2952.
- [23] C. V. Yelamaggad, A. S. Achalkumar, D. S. S. Rao, M. Nobusawa, H. Akutsu, J. Yamada, S. Nakatsuji, *J. Mater. Chem.* **2008**, *18*, 3433–3437.
- [24] S. Castellanos, D. Velasco, F. López-Calahorra, E. Brillas, L. Julia, *J. Org. Chem.* **2008**, *73*, 3759–3767.
- [25] O. Armet, J. Veciana, C. Rovira, J. Riera, J. Castañer, E. Molins, J. Rius, C. Miravittles, S. Olivella, J. Brichfeus, *J. Phys. Chem.* **1987**, *91*, 5608–5616.
- [26] D. Velasco, S. Castellanos, M. Lopez, F. Lopez-Calahorra, E. Brillas, L. Julia, *J. Org. Chem.* **2007**, *72*, 7523–7532.
- [27] V. Gamero, D. Velasco, S. Latorre, F. Lopez-Calahorra, E. Brillas, L. Julia, *Tetrahedron Lett.* **2006**, *47*, 2305–2309.
- [28] S. Laschat, A. Baro, N. Steinke, F. Giesselmann, C. Haegel, G. Scalia, R. Judele, E. Kapatsina, S. Sauer, A. Schreivogel, M. Tosoni, *Angew. Chem.* **2007**, *119*, 4916–4973; *Angew. Chem. Int. Ed.* **2007**, *46*, 4832–4887.
- [29] H. Iino, J. Hanna, R. J. Bushby, B. Movaghar, B. J. Whitaker, *J. Appl. Phys.* **2006**, *100*, 043716.
- [30] P. Bauer, H. Wietasch, S. M. Lindner, M. Thelakkat, *Chem. Mater.* **2007**, *19*, 88–94.
- [31] M. Ballester, *Adv. Phys. Org. Chem.* **1989**, *25*, 267–445.